Microscopic explanation of the shape-phase transition at $N = 88$–90 and the $Z = 64$ subshell effect for Ba–Dy

J. B. Gupta*
Ramjas College, University of Delhi, Delhi 110007, India
(Received 6 April 2013; published 26 June 2013)

Background: The shape-phase transition at $N = 88$–90, and the role of $Z = 64$ subshell effect therein has been a subject of study on empirical basis and in the context of the N_pN_n scheme, but a microscopic view of the same has been lacking.
Purpose: A microscopic view of the $N = 88$–90 shape-phase transition is developed. The $Z = 64$ subshell effect is viewed in terms of the Nilsson single-particle orbitals in this region.
Method: The dynamic pairing plus quadrupole model is employed to predict the occupation probabilities of the neutron and proton deformed, single-particle orbitals. The nuclear structure of Ba–Dy ($N > 82$) nuclei is studied and the shape equilibrium parameters derived.
Results: The filling of neutron orbitals at $N = 86$, 88, and 90 plays an important role in the shape-phase transition. The filling of the proton Nilsson orbitals of varying slopes leads to the variation of nuclear structure with varying Z, which leads to the $Z = 64$ subshell effect, which disappears at $N = 90$.
Conclusions: The effect of the n-p interaction of the $\pi h_{11/2}$ and $\nu h_{9/2}$ orbitals, along with the contribution of the $\nu i_{13/2}$ orbital leads to the shape-phase transition at $N = 88-90$. The slopes of proton Nilsson orbitals explain the $Z = 64$ subshell effect.

DOI: 10.1103/PhysRevC.87.064318 PACS number(s): 21.60.Ev, 21.10.Jx, 21.10.Re, 27.70.+q

I. INTRODUCTION

In the study of collective nuclear structure of atomic nuclei, the phenomenon of shape-phase transition with the addition of protons or neutrons has been of great interest for a long time. The shape transition at $N = 88$–90 was noted in the early 1950s by Mottelson and Nilsson [1]. While for $N = 88$, ^{150}Sm and ^{152}Gd are considered to be spherically symmetric, for $N = 90$, ^{152}Sm and ^{154}Gd exhibit the features of a soft deformed rotor.

The empirical study of the energy levels in the ground-state band of even-Z–even−N nuclei enables us to distinguish the vibratorlike spectra from the rotorlike. These regular spectra led Bohr and Mottelson to propose the quantum mechanical version of the collective model of nuclei (BM model) [2], different from the independent particle shell model.

Soon it was realized that most of the other nuclei between these limiting symmetries have an intermediate character. The energy $E(2_1{}^+)$ or the inverse $3/E(2_1{}^+) =$ moment of inertia (MoI) provides the first information, which varies with N and Z. The energy ratio $R_{4/2}(= E_4/E_2)$, which is independent of the mass effect on account of the cancellation of the MoI term, provides another useful observable which can be used for all nuclei, which display the collective spectra. In the study of the rare–earth-metal region [3], the plot of the energy ratio $R_{4/2}$ versus atomic number Z for different neutron numbers N showed interesting features, the most important being the shape-phase transition at $N = 88-90$, which also illustrates the $Z = 64$ subshell effect. The transition at $N = 88$–90 is maximum for $Z = 64$ Gd isotopes, which tapers off on both sides of $Z = 64$.

In the context of the interacting boson model, IBM-1 and IBM-2 [4], the counting of nucleon pair numbers assumed new significance, and the determination of the effective subshell became necessary. Casten *et al.* discussed the $Z = 64$ subshell effect for $N \leqslant 88$ isotones, which, however, disappears at $N = 90$ [5]. Also a Z-dependent effect has to be taken into account. Proper methods of estimating the subshell effects have been reported [6,7]. In terms of the Nilsson deformed single-particle model, the smallness of the subshell gap ΔE between $(g_{7/2}d_{5/2})$ and $h_{11/2}$ subshells was studied earlier in Ref. [8]. Recently, a microscopic explanation of the isotonic multiplets, with almost identical spectra, at $N = 90$ was given in Ref. [9]. Here, we focus on the variation of nuclear structure at $N = 86$ and $N = 88$ with varying Z, producing the $Z = 64$ subshell effect. Besides the empirical picture, we present a microscopic view of the situation in terms of the Nilsson single-particle deformed orbits and their filling with neutrons and protons.

In Sec. II we present empirical evidence of the shape-phase transition and the $Z = 64$ subshell effect. The role of Nilsson single-particle orbits is illustrated. In Sec. III, a brief description of the dynamic pairing plus quadrupole (DPPQ) model and of the spectroscopic factors is given. In Sec. IV, details of the calculation and results are given. Summary and discussion are given in Sec. V.

II. SHAPE-PHASE TRANSITION

A. Empirical data

For the $Z = 50$–82 shell, normally the energy $E(2_1)$ for a given isotonic series should decrease with increasing number of valence protons, with a minimum at midshell $Z = 66$, and increase thereafter with decreasing number of proton-hole

*jbgupta2011@gmail.com

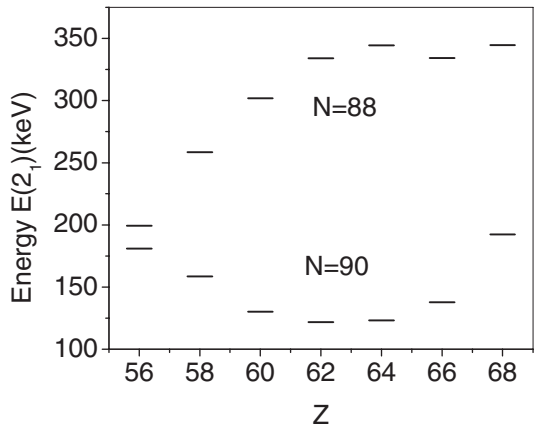

FIG. 1. Level energy $E(2_1{}^+)$ in ground band of Ba–Er. Maximum rise and fall are at $Z = 64$ Gd.

pairs. In Fig. 1, the level energy $E(2_1{}^+)$ [10] is plotted versus the atomic number Z. The values for $N = 90$ isotones are low, corresponding to the soft deformed rotor. Also, the values for Nd, Sm, Gd, and Dy are almost the same. But the values for $N = 88$ exhibit the opposite trend, with a sharp rise towards $Z = 66$, the maximum effect being at $Z = 64$ Gd. Here the values for Sm, Gd, Dy, and Er are similar, but there is some variation for $Z = 56$–60. The value of $E(2_1)$ for Ba, Ce, and Nd are lower. In Ba the values for $N = 88$, 90 differ by only 20 keV.

The same behavior is seen in the values of the energy ratio $R_{4/2}$ $(= E_4/E_2)$ in Fig. 2. A peak is formed at $N = 90$ (Nd, Sm, Gd, Dy) isotones, and a valley is formed at $N = 88$ isotones of (Sm, Gd, Dy). Variation with Z in $N = 86$ isotones is similar. In Ba, a larger transition occurs at $N = 86$–88. Casten *et al.* [5] explained this behavior of $N \leqslant 88$ isotones on the basis of the $Z = 64$ subshell effect.

B. The $Z = 64$ subshell effect

If the subshell effect is active, the effective number N_p of valence proton pairs decreases as one approaches $Z = 64$ (yielding $N_p = 0$). It is also apparent that the number N_p should not vary so drastically, but vary rather more smoothly.

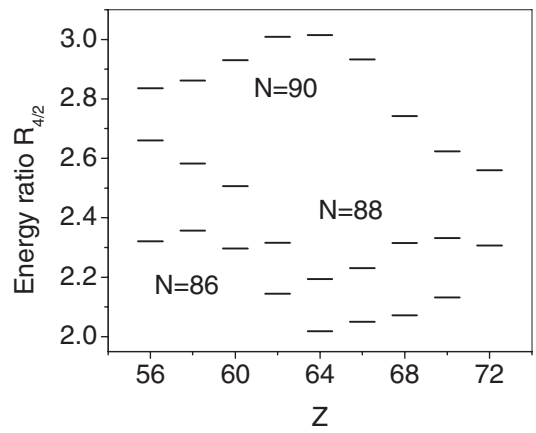

FIG. 2. Energy ratio $R_{4/2}(= E_4/E_2)$ versus Z for $N = 86$, 88, and 90 isotones of Ba–Hf.

Using the $B(E2)$ and $g(2_1)$ data, Wolf *et al.* [7] estimated the effective numbers of N_p and N_n valence nucleon pairs or hole pairs. This enabled a linear relation of $B(E2)$ and $g(2_1)$ with the product N_pN_n, the latter being a good measure of the deformation. In the empirical approach of the N_pN_n scheme [11], such an approach is very useful and gives an idea of the complexity of the underlying structure. It is also evident from Figs. 1 and 2, as also discussed in the literature [5–7,11], that the $Z = 64$ subshell effect disappears at $N \geqslant 90$.

In the independent particle shell model view, the $g_{7/2}$ subshell fills at $Z = 58$ and the $d_{5/2}$ subshell fills at $Z = 64$, with the next subshell being of the intruder $\pi h_{11/2}$. Guided by the odd-A nuclei data structures, Nilsson *et al.* [12] suggested a level spacing pattern (at $\beta = 0$), as also adopted in Ref. [2]. The $\pi d_{5/2}$ spacing is about 0.8 MeV and $\pi h_{11/2}$ subshell lies at 1.0 MeV higher. So the $Z = 64$ subshell closure effect is rather weak. The absence of excited states in the $E = 166$–1200 keV interval in $^{139}La_{82}$ indicates that the seven protons fill the $g_{7/2}$ at $N = 82$. The stripping and pickup reactions [13] in $N = 82$ isotones of $_{53}$I to $_{63}$Eu showed 80% occupancy of $g_{7/2}$ and $d_{5/2}$ orbits in ^{144}Sm, in conformity with the slightly larger $d_{5/2}h_{11/2}$ energy gap.

To resolve the ambiguity of the subshell gap ΔE, in a previous microscopic analysis [8], the $Z = 64$ subshell gap at the spherical limit was studied. It was found that the $Z = 64$ subshell gap is rather small, which can be wiped out at larger deformation. The usual explanation for this disappearance of the subshell gap is in terms of the relatively stronger n-p interaction, when there is a spin-orbit partnership between the valence neutrons and protons [11]. In the present case, the protons filling the $\pi h_{11/2}$ orbits and the neutrons in the $\nu h_{9/2}$ orbits produce an attractive influence, thereby decreasing the effective subshell gap [5,7,11]. It will be useful to study these effects in greater detail. Especially, we analyze the mechanism generating the well visible $Z = 64$ subshell gap in the plots of Figs. 1 and 2. We focus on the structural changes at $N = 86$, 88 in Ba–Gd and Dy.

C. Nilsson single-particle orbits

The approach in the present study is to illustrate the role of the single-particle Nilsson orbits in this region and the occupation of these orbits by the nucleons, varying with N, Z. For this purpose, we illustrate the deformed single-particle Nilsson orbits for $Z > 50$ protons and $N > 82$ neutrons. The energy scale is in units of $\hbar\omega$, one unit ~8 MeV.

One can see in Fig. 3 for neutrons that at small quadrupole deformation β, for $N = 84$, 86, two and four valence neutrons can occupy the two down-sloping orbits of the $f_{7/2}$ subshell. At $N = 88$, the two additional neutrons can fill the down-sloping $\Omega = 1/2$ $h_{9/2}$ orbit. But at $N = 90$, the low Ω orbit of the intruder $\nu i_{13/2}$ subshell would fill along with the one of $\nu h_{9/2}$ and two of $\nu f_{7/2}$ orbits. In fact, with increasing deformation, there can be a transfer of neutrons from the $\nu f_{7/2}$ subshell to $\nu h_{9/2}$ subshell and the close-lying intruder $i_{13/2}$ subshell. The increasing deformation with increasing number of neutrons would affect this simple picture.

Next we look at the proton orbits in Fig. 4. For small deformation, the three proton pairs of Ba ($Z = 56$) should

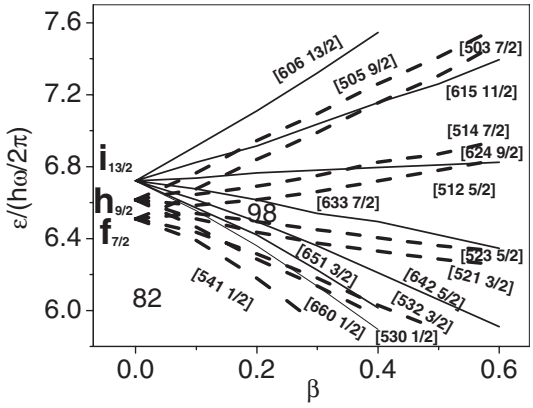

FIG. 3. Neutron Nilsson orbits for $N.>.82$, adopted from [2,9].The energy scale is in units of $\hbar\omega$.

fill two orbits of the $\pi g_{7/2}$ subshell and one of $d_{5/2}$ subshell. At spherical limit, additional proton pairs in Ce and Nd would fill the horizontal $\pi[413, 5/2]$ and $\pi[411\ 3/2]$ orbits of $g_{7/2}$ and $d_{5/2}$ subshells, respectively. The proton pairs of Sm and Gd would fill the up-sloping [404 7/2] and [402 5/2] orbits of $\pi g_{7/2}$ and $\pi d_{5/2}$. It is apparent that the increasing protons lead to a lesser deformation, and this will be more effective for $N = 86$ and less for $N = 88$ on account of deformation. This is the static view. In a dynamic view, *due to the pairing interaction*, these numbers would change on account of the partial filling of the single-particle orbits.

III. THEORY

A. Dynamic pairing plus quadrupole model

The dynamic pairing plus quadrupole (DPPQ) model of Kumar-Baranger [14,15] is well suited to estimating the *spectroscopic factors* of neutrons and protons in deformed single-particle Nilsson orbits for shape transitional nuclei. Only a brief introduction of the model is given here (see [15] and references cited therein).

With an inert core of $Z = 40$ and $N = 70$, it includes all valence nucleons in the $N = 4$, 5 and $N = 5$, 6

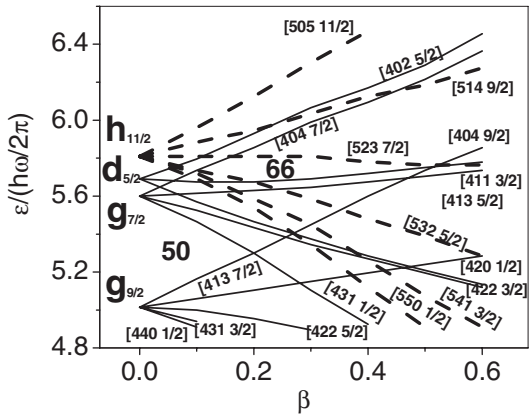

FIG. 4. Proton Nilsson orbits for $Z >.40$, adopted from [2,9]. The energy scale is in units of $\hbar\omega$.

spherical harmonic oscillator shells for protons and neutrons respectively (21 proton orbits and 28 neutron orbits). It is a fully self-consistent dynamic theory and treats the quadrupole and pairing interactions on an equal footing. It employs the well-known generalized Hartree-Bogoliubov (GHB) technique. Employing the harmonic oscillator basis, the quadrupole interaction is added to obtain the deformed single-particle basis (dsp). Then the pairing interaction is used in the BCS technique, which yields the deformed quasiparticle basis (dqp).

A triangular mesh of 92 points in collective variables (β, γ) is employed with ($\beta = 0$ to 0.5, $\gamma = 0^\circ$ to 60°). The dqp solutions are obtained for all the mesh points, and the collective model parameters are determined at all points. No assumption is made regarding the shape of the nucleus, and it allows the nucleus to take its own shape, with full freedom in the (β, γ) space. The updated, efficient solution method for $H_{\rm PPQ}$ reviewed in [15] is employed in the present work. In the last four decades, we have applied the DPPQ model for the study of the collective structures of nuclei in $A = 150$–200 region of Nd–Dy. For example, see [16–19] and other references cited therein.

The DPPQ model was also used for the calculation of the spectroscopic factors for protons in $^{148-154}$Sm [20] and $N = 88$, 90 Nd, Sm, Gd isotones [9,21]. For the present purpose, we have solved the DPPQ Hamiltonian for Ba and Ce $N = 86$, 88, 90 isotones, and $N = 86$ Nd–Dy isotones. The results from the earlier study of $N = 90$ and $N = 88$ for Nd–Dy in [9,20,21] are adopted here for a full description of the filling of Nilsson orbits.

B. Spectroscopic factors

In the spherical quasiparticle model, for the pickup from an even-even target nucleus, the spectroscopic factor is defined as

$$S_a^- = (2j_a + 1)\, v_a^2, \tag{1}$$

where a is a composite index for the nucleon quantum numbers ($a \cong \tau, n, l, j$) and ${v_i}^2$ is the occupation probability of the single-particle level a, or

$$S_a^- = (2j_a + 1)\, v_a^2 = (2j_a + 1)\rho_{aa}, \tag{2}$$

TABLE I. Single-particle proton and neutron orbit energies at $\beta = 0$, in units of $\hbar\omega$, employed for the DPPQ model calculation, adopted from [14]. For protons $N = 4$, 5 and neutrons $N = 5$, 6.

Orbital	Energy	Orbital	Energy	Orbital	Energy	Orbital	Energy
$1g_{9/2}$	−0.975	$1h_{11/2}$	−0.150	$1h_{11/2}$	−1.202	$1i_{13/2}$	−0.300
$1g_{7/2}$	−0.300	$1h_{9/2}$	+0.575	$1h_{9/2}$	−0.430	$1i_{11/2}$	+0.500
$2d_{5/2}$	−0.265	$2f_{7/2}$	+0.620	$2f_{7/2}$	−0.475	$2g_{9/2}$	+0.445
$2d_{3/2}$	−0.015	$2f_{5/2}$	+0.970	$2f_{5/2}$	−0.125	$2g_{7/2}$	+0.895
$3s_{1/2}$	0.0	$1p_{3/2}$	+0.995	$1p_{3/2}$	−0.150	$3d_{5/2}$	+0.860
		$1p_{1/2}$	+1.145	$1p_{1/2}$	0.0	$3d_{3/2}$	+1.110
						$4s_{1/2}$	+1.095

TABLE II. Parameters of the DPPQ model for $N = 86$ isotones. All other parameters are kept constant. Derived values of $\beta_{\min}$, $\beta_{0\text{rms}}$, and $\gamma_{0\text{rms}}$ at ground state are listed.

Parameter	Ba	Ce	Nd	Sm	Gd	Dy
X_0 MeV^{-1}	76.0	76.0	73.5	70.5	70.0	70.0
F_B	3.0	3.0	2.6	2.6	2.4	2.40
$\beta_{\min}$	0.0	0.0	0.0	0.0	0.0	0.0
$\beta_{0\text{rms}}$	0.155	0.166	0.168	0.153	0.154	0.152
$\gamma_{0\text{rms}}$	25.8°	21.0°	24.0°	26.0°	26.0°	26.5°

where ρ_{aa} is the density matrix. In a quasistatic approximation, we calculate $\rho_{\alpha\alpha}$ for the average value of deformation and the average ρ over the magnetic quantum numbers. This yields the expression for ρ_{aa}

$$\rho_{aa} = v_a^2 = (2j_a + 1)^{-1} \Sigma_{m_\alpha} \rho_{\alpha\alpha}, \tag{3a}$$

$$\text{where } \rho_{\alpha\alpha} = \Sigma_i v_i^2 \langle \alpha | i \rangle^2 . \tag{3b}$$

And $\langle \alpha | i \rangle^2$ is the probability that the spherical state $|\alpha\rangle$ is contained in the deformed state $|i\rangle$. We employ the combination of Eqs. (2) and (3).

IV. CALCULATION AND RESULTS

A. Parameters of DPPQ model

As described above, in the DPPQ model we start with single-particle energies at $\beta = 0.0$ and harmonic oscillator wave functions. The single-particle energies of Ref. [14] employed in our work are listed in Table I. The subshell gap at $\pi(g_{7/2}$–$d_{5/2})$ is small here, but the $\pi h_{11/2}$ subshell lies higher at about 1.0 MeV. Similarly, the intruder subshell of $\nu i_{13/2}$ lies higher. A detailed discussion of the subshell gap is given in Ref. [8].

The quadrupole force strength constant is written as

$$X = X_0 A^{-1.4}. \tag{4}$$

Here the normal value of X_0 is 70.0 MeV^{-1}. This is allowed to vary by a few percent to reproduce the experimental spectrum. Also, to take into account the effect of the $Z = 40$, $N = 70$ inert core, the inertial coefficients are multiplied by a common factor of 2.0–3.0. The values employed for the present work are given for $N = 86$, 88, and 90 isotones in Tables II, III, and IV respectively. These values lie in the stated range.

TABLE III. Parameters of the DPPQ model for $N = 88$ isotones and derived $\beta_{\min}$, $\beta_{0\text{rms}}$, and $\gamma_{0\text{rms}}$.

Parameter	Ba	Ce	Nd	Sm	Gd	Dy
X_0 MeV^{-1}	75.0	72.5	70.5	70.0	67.5	69.5
F_B	2.6	2.6	2.45	2.0	3.0	2.15
$\beta_{\min}$	0.205	0.205	0.205	0.205	0.174	0.205
$\beta_{0\text{rms}}$	0.206	0.200	0.194	0.200	0.164	0.192
$\gamma_{0\text{rms}}$	18.7°	19.1°	20.0°	20.0°	19.0°	20.2°

TABLE IV. Parameters of the DPPQ model for $N = 90$ isotones and derived $\beta_{\min}$, $\beta_{0\text{rms}}$, and $\gamma_{0\text{rms}}$.

Parameter	Ba	Ce	Nd	Sm	Gd	Dy
X_0 MeV^{-1}	71.0	71.0	69.5	70.0	70.0	69.5
F_B	2.5	2.2	2.7	2.2	2.4	2.1
$\beta_{\min}$	0.205	0.236	0.236	0.236	0.236	0.236
$\beta_{0\text{rms}}$	0.218	0.245	0.24	0.258	0.262	0.252
$\gamma_{0\text{rms}}$	17.0°	15.6°	15.0°	14.7°	13.7°	14.7°

B. The $N = 86$ isotones

At $N = 86$, with only four valence neutrons, the Ba–Dy isotones do not have a well-developed K-band structure [10]. The energy ratio varies from 2.0 to 2.2. Here the energy levels can be viewed in terms of one phonon singlet, two phonon triplet (and $N = 3$ quintuplet), corresponding to an anharmonic vibrator. We have solved the DPPQ model Hamiltonian for the $N = 86$ isotones. The potential energy surface $V(\beta, \gamma)$ has a minimum at $\beta = 0$, but the β_{rms} value at ground state is nonzero and is about 0.15 (Table II), indicating the anharmonic vibrator structure. As stated above, in the DPPQ model, one can vary the quadrupole strength constant X_0 by a few percent about the initial value of 70.0. Also the initial value of the inert core renormalization factor F_B of 2.4 can be varied by a small amount to approximately get $E(2_1)$ and ratio $R_{4/2}$ [17,18]. Thus in the present work, we have reproduced the basic level structures of the $N = 86$ isotones of Ba–Dy. Then using the corresponding X_0 and F_B values and the potential minimum deformation value, we have calculated the spectroscopic factors and the occupation numbers of neutrons and protons in these nuclei. The same are listed in Tables V and VI. In the tables, we have omitted the numbers for $\pi g_{9/2}$ and $\nu h_{11/2}$, which are nearly fully occupied, and ones for the other orbits, scantly occupied. The sums for these listed orbits represent 80–90% of the full values.

The four valence neutrons above $N = 82$ are distributed over the orbits of $f_{7/2}$, $h_{9/2}$, and $i_{13/2}$, which lie lowest and are closely held (see Fig. 3 and Table I). This distribution is almost the same for all Z (Table V). The four neutrons do not produce a static deformed shape; though the dynamics of nucleon motion does provide some anharmonicity ($\beta_{\text{rms}} > 0$).

The increasing valence protons in Ba–Dy (6 to 16) mainly fill the $g_{7/2}$, $d_{5/2}$, and $h_{11/2}$ orbits successively. The increasing filling of down-sloping orbits (Table VI) provides a small

TABLE V. Occupation numbers of neutrons in Nilsson orbits at $\beta = 0$ for $N = 86$ isotones of $Z = 56$–66, calculated in the DPPQ model [14,15].

Subshell	Ba	Ce	Nd	Sm	Gd	Dy
$\nu f_{7/2}$	1.688	1.686	1.684	1.682	1.607	1.680
$\nu h_{9/2}$	1.400	1.400	1.399	1.400	1.407	1.398
$\nu i_{13/2}$	0.713	0.715	0.717	0.718	0.355[a]	0.720
Sum	3.801	3.801	3. 800	3.800	3.369	3.798

[a]A low occupancy is predicted, the rest being shared by other orbitals $f_{5/2}$, $p_{3/2}$.

TABLE VI. Occupation numbers of protons in Nilsson orbits at $\beta = 0$ for $N = 86$ isotones of $Z = 56$–66, calculated in the DPPQ model.

Subshell	Ba	Ce	Nd	Sm	Gd	Dy
$\pi g_{7/2}$	2.609	3.352	4.038	4.665	4.788	5.742
$\pi d_{5/2}$	1.560	2.065	2.559	3.036	3.106	3.917
$\pi h_{11/2}$	1.470	2.035	2.657	3.345	4.586	4.940
Sum	5.639	7.452	9.254	11.047	12.480	14.699

gradual change in the level energy and Z dependence (Figs. 1 and 2). The filling of the protons has the same trend as cited above for $N = 82$ closed-shell isotones. However, it may be noted that increasing filling of protons beyond Ba in Ce, Nd, Sm, and Gd implies the filling of the almost horizontal π[413, 5/2] and π[411 3/2] orbits at zero or small deformation. This has the effect of a closed $Z = 64$ subshell. The small number of neutrons at $N = 86$ keeps the deformation small.

C. The $N = 88$ isotones

The calculated occupation numbers of neutrons and protons from the DPPQ model for $N = 88$ isotones are listed in Tables VII and VIII, respectively. Only the values for ($\nu f_{7/2}$, $\nu h_{9/2}$, $\nu i_{13/2}$) for neutrons and for ($\pi g_{7/2}$, $\pi d_{5/2}$, $\pi h_{11/2}$) for protons are given here. At $N = 88$, the two additional neutrons fill the $f_{7/2}$ and $h_{9/2}$ orbits which give rise to a small deformation ($\beta_{\min} = 0.20$) in $N = 88$ isotones ($\beta_{\min} = 0.174$ for Gd, see Table III). The neutron occupation at $N = 88$ (Table VII) is not affected by the filling of protons, as for $N =$ 86 isotones.

An increasing number of protons occupy the g, d, and h subshells for Ba–Dy. The quadrupole deformation sets in Ba earlier at $N = 86$–88, in which only down-sloping orbits are effective. This is expected from the $E(2_1)$ and $R_{4/2}$ plots in Figs. 1 and 2. Scott *et al.* [22] noted the onset of deformation in Ba, at $N = 86$–88. The filling of (g, d) subshell increases with increasing Z. But as for $N = 86$ isotones, for the small deformation here, too, the additional protons go to horizontal orbits π[413, 5/2] and π[411 3/2], which restrict the effect of the increasing filling of $h_{11/2}$ low-Ω orbits. Again this has the net effect of the observed $Z = 64$ subshell.

TABLE VII. Occupation numbers of neutrons in Nilsson orbits at $\beta = 0.205$ for $N = 88$ isotones (0.174 for Gd) of $Z = 56$–66 in quadrant 1, calculated in the DPPQ model.

Subshell	Ba	Ce	Nd	Sm	Gd	Dy
$\nu f_{7/2}$	2.013	2.016	2.02	2.02	2.12	2.02
$\nu h_{9/2}$	2.183	2.182	2.18	2.18	2.17	2.18
$\nu i_{13/2}$	0.631	0.635	0.64	0.64	0.72	0.65
Sum	4.827	4.833	4.84	4.84	5.01	4.93
$N = 82$	6	6	6	6	6	6

TABLE VIII. Occupation numbers of protons in Nilsson orbits at $\beta = 0.205$ for $N = 88$ isotones (0.174 for Gd) of $Z = 56$–66 in quadrant 1, calculated in the DPPQ model.

Subshell	Ba	Ce	Nd	Sm	Gd	Dy
$\pi g_{7/2}$	2.508	3.109	3.65	4.16	4.79	5.15
$\pi d_{5/2}$	1.536	1.915	2.27	2.63	3.11	3.35
$\pi h_{11/2}$	1.316	2.082	2.95	3.84	4.58	5.65
Sum	.5.360	7.106	8.87	10.63	12.48	14.15
Z-50	6	8	10	12	14	16

D. The $N = 90$ isotones

At $N = 90$, the two additional neutrons occupy the $h_{9/2}$ and $i_{13/2}$ orbits. This leads to a greater deformation effect compared to the $N = 86, 88$ case. In the present work, we have calculated the spectroscopic factors for Ba and Ce isotones. The occupation numbers for neutrons and protons in Ba, Ce, and Nd–Dy (from previous work [9]) for $N = 90$ are cited in Tables IX and X. The data in Table IX show that beyond the $N = 82$ closed shell, the filling of the neutrons in $\nu f_{7/2}$, $\nu h_{9/2}$, and $\nu i_{13/2}$ subshells remains almost constant for varying Z. The equilibrium quadrupole deformation $\beta_2 = 0.236$ is also constant except for Ba, where it reduces to 0.205. This is in accord with the relatively less deformed structure of ^{146}Ba as exhibited in Figs. 1 and 2. The eight valence neutrons play the main role in producing the deformation at $N = 90$, as evident in Figs. 1 and 2 for $E(2_1)$ and $R_{4/2}$.

From Table X, it is apparent that the increasing number of valence protons beyond the $Z = 50$ closed shell fill the three subshells of $\pi g_{7/2}$, $\pi d_{5/2}$, and $\pi h_{11/2}$. The increasing filling of the $\pi h_{11/2}$ subshell, which has the n-p spin-orbit partnership with $\nu h_{9/2,}$ is especially effective in producing the deformation at $N = 90$ and the resulting shape-phase transition. The $Z = 64$ subshell effect is wiped out at $N = 90$ and the resulting larger deformation equilibrium point, which alters the distribution of the protons across the (g, d, and h) orbits.(see the crossing of orbits of $h_{11/2}$ into those of g, d orbits).

In Ref. [9], we have also explained the constancy of structure of $N = 90$ isotones of Nd–Dy on account of the filling of the almost horizontal Nilsson orbits π [413, 5/2] and π[411 3/2] of $\pi g_{7/2}$ and $\pi d_{5/2}$ subshells, respectively, forming the $N = 90$ isotonic multiplet. This is also reflected in the broad peak at Sm–Dy in Fig. 2 for $R_{4/2}$. The much smaller number of protons in Ba provides lesser deformation.

TABLE IX. Occupation numbers of neutrons in Nilsson orbits at $\beta = 0.236$ for $N = 90$ isotones (0.205 for Ba) of $Z = 58$–66 in quadrant 1, calculated in the DPPQ model [14,15].

Subshell	Ba	Ce	Nd	Sm	Gd	Dy
$\nu f_{7/2}$	2.419	2.282	2.29	2.29	2.29	2.30
$\nu h_{9/2}$	2.761	2.681	2.68	2.69	2.69	2.69
$\nu i_{13/2}$	1.324	1.451	1.45	1.44	1.44	1.43
Sum	6.504	6.414	6.42	6.42	6.42	6.42

TABLE X. Occupation numbers of protons in Nilsson orbits at $\beta = 0.236$ for $N = 90$ isotones (0.205 for Ba) of $Z = 58$–66 in quadrant 1, calculated in the DPPQ model.

Subshell	Ba	Ce	Nd	Sm	Gd	Dy
$\pi g_{7/2}$	2.512	3.039	3.54	4.04	4.54	5.03
$\pi d_{5/2}$	1.537	1.859	2.18	2.52	2.88	3.25
$\pi h_{11/2}$	1.309	2.144	3.07	4.00	4.90	5.78
Sum	5.358	7.042	8.79	10.56	12.32	14.06

E. The $N = 88$–90 shape-phase transition

To better appreciate the role of neutron and proton occupation numbers we have plotted these numbers for 88, 90 in Fig. 5 (neutrons) and Figs. 6 and 7 (protons). Note the sharp rise at $N = 88$–90 for $\nu i_{13/2}$ (filled and open circles) and for $\nu h_{9/2}$ (cross and plus symbols) (Fig. 5). Figure 6 for protons at $N = 88$ and Fig. 7 for $N = 90$ illustrate the increasing filling numbers of protons in $d_{5/2}$(plus symbol) and $g_{7/2}$ (upright triangle symbol). The filling in $\pi h_{11/2}$ orbits overtakes $g_{7/2}$ at $Z = 62$ Sm (Fig. 7). However, the effects of the slopes of the Nilsson orbits are not evident in these plots (Figs. 5–7), which cause the $Z = 64$ subshell effects and the formation of isotonic multiplets.

Besides the n-p attraction of spin-orbit partners of $\pi h_{11/2}$ and $\nu h_{9/2}$ which is a well-recognized effect, our study also illustrates the role of $\nu i_{13/2}$ subshell down-sloping orbits which assist the shape transition at $N = 88$–90. The occupancy of the lower subshells listed here is more than 80%, thus accounting for the major effects. In Fig. 5 for the occupation numbers of neutrons, the role of the $h_{9/2}$ (+ and × symbols) and $i_{13/2}$ (open and filled circles) in inducing the $N = 88$–90 shape-phase transition is transparently visible. In each of these subshells, the occupation numbers increase by about one unit (see Fig. 5).

V. DISCUSSION AND CONCLUSION

In the language of the collectivity (deformation) depending on the number of valence nucleons, it was rightly concluded [5–7] that the $Z = 64$ subshell effect comes into play to change the effective N_p, N_n numbers. The slightly greater deformation induced by $\nu h_{9/2}$ neutrons in the down-sloping orbits will affect a transfer of active proton pairs from the aforesaid up-sloping orbits to the down-sloping low-Ω orbits of the $h_{11/2}$ subshell. It may be noted that this simple picture is modified slightly due to the scattering of nucleons due to the pairing interaction. As per the study of the $Z = 64$ subshell gap being small [2,8], the gap is effective only at the spherical or small deformation limit. As soon as some deformation takes place, there is a builtin tendency to alter the situation from a decreasing deformation to an increasing deformation. What was deduced from empirical analysis is well supported by the microscopic view in terms of the filling of Nilsson orbitals of protons and neutrons developed here. The difference lies mainly in the language used in the two views, the empirical and the microscopic. In the former view, the emphasis is on deducing the effective numbers, while in the latter it is on the slopes of the Nilsson orbitals and competitive filling of the ($g_{7/2}$, $d_{5/2}$) and $h_{11/2}$ subshells. Here we may note that the formation of isotonic multiplets at $N = 90$, as explained microscopically in Ref. [9], rested on the involvement of the two almost horizontal orbits [413 5/2] and [411 3/2] for

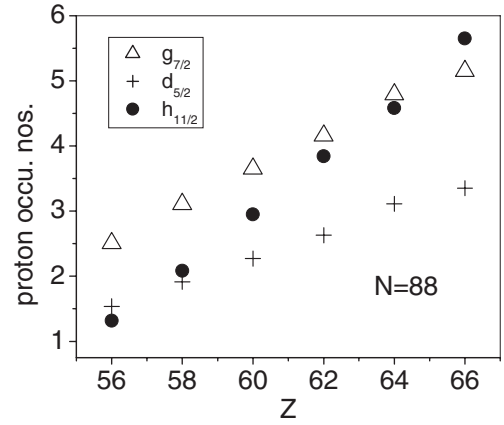

FIG. 6. Proton occupation numbers in deformed single-particle Nilsson subshells at $N = 88$ from DPPQ model.

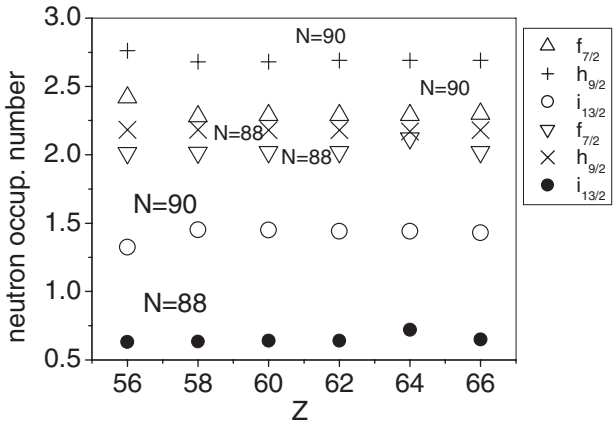

FIG. 5. Occupation numbers of neutrons in deformed Nilsson single-particle subshells from DPPQ model (see text).

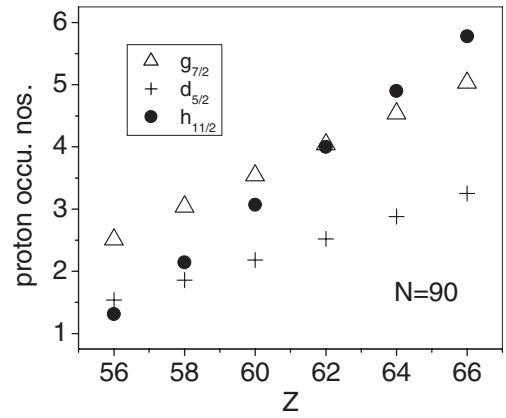

FIG. 7. Proton occupation numbers in deformed single-particle Nilsson subshells at $N = 90$, from DPPQ model.

protons of (Sm, Gd, Dy). Also, the role of the $\nu i_{13/2}$ subshell is pointed out here.

The increasing $R_{4/2}$ for $N = 86$, 88 and decreasing value at $N = 90$ isotones of Er, Yb, and Hf (Fig. 2) can also be understood in terms of the filling of the protons at differing deformation points in the respective cases. Beyond $Z = 66$, even at small deformation, the additional proton pairs of Er, Yb, and Hf fill the $h_{11/2}$ subshell. At larger deformation (at $N = 90$), these additional proton pairs fill the up-sloping orbits, inducing decreasing $R_{4/2}$ (see Fig. 2).

At the microscopic level, one can visualize the variation of nuclear structure with N, Z in terms of the Nilsson single-particle orbitals and their slopes. On account of the small gap between the $Z = 64$ filled (g, d) subshells and the intruder $h_{11/2}$ subshell, the sharing of active nucleons between them is profoundly affected by the filling of neutrons in the $h_{9/2}$ subshell. This phenomenon was rightly ascribed to the p-n interaction. Here we have gone deeper in terms of the filling of Nilsson orbits, which makes the picture more transparent and illustrates the role of the $\nu i_{13/2}$ subshell as well.

ACKNOWLEDGMENT

J.B.G. appreciates the association with Ramjas College, University of Delhi, and the support from Dr. Rajendra Prasad.

[1] B. R. Mottelson and S. G. Nilsson, Phys. Rev. **99**, 615 (1955).
[2] A. Bohr and B. R. Mottelson, *Nuclear Structure*, Vol. II (Benjamin, New York, 1975).
[3] J. B. Wilhelmy, S. G. Thomson, R. C. Javed, and E. Chieftez, Phys. Rev. Lett. **25**, 1122 (1970).
[4] A. Arima and F. Iachello, *The Interacting Boson Model* (Cambridge University, New York, 1987).
[5] R. F. Casten, D. D. Warner, D. S. Brenner, and R. L. Gill, Phys. Rev. Lett. **47**, 1433 (1981).
[6] R. L. Gill, R. F. Casten, D. D. Warner, D. S. Brenner, and W. B. Walters, Phys. Lett. B **118**, 251 (1983).
[7] A. Wolf and R. F. Casten, Phys. Rev. C **36**, 851 (1987).
[8] J. B. Gupta, Phys. Rev. C **47**, 1489 (1993).
[9] J. B. Gupta, Eur. Phys. J. A **48**, 177 (2012).
[10] Brookhaven National Laboratory, Chart of nuclides of National Nuclear Data Center http://www.nndc.bnl.gov/ensdf.
[11] R. F. Casten, Nucl. Phys. A **443**, 1 (1985).
[12] S. G. Nilsson, C. F. Tsang, A. Sobiczewski, Z. Szymanski, S. Wycech, C. Gustafson, I. L. Lamm, P. Moller, and B. Nilsson, Nucl. Phys. A **131**, 1 (1969).
[13] B. H. Wildenthal, E. Newman, and R. L. Auble, Phys. Rev. C **3**, 1199 (1971).
[14] K. Kumar and M. Baranger, Nucl. Phys. A **110**, 529 (1967).
[15] K. Kumar, in *The Electromagnetic Interaction in Nuclear Spectroscopy*, edited by W. D. Hamilton (North-Holland, Amsterdam, 1975), Chap. 3.
[16] K. Kumar, J. B. Gupta, and J. H. Hamilton, Aust. J. Phys. **32**, 307 (1979).
[17] J. B. Gupta, Phys. Rev. C **28**, 1829 (1981).
[18] J. B. Gupta, Phys. Rev. C **39**, 1604 (1989).
[19] J. B. Gupta, K. Kumar, and J. H. Hamilton, Int. J. Mod. Phys. E **19**, 2591 (2010).
[20] K. Kumar, J. B. Gupta, and J. H. Hamilton, Nucl. Phys. A **448**, 36 (1986).
[21] J. B. Gupta and S. Sharma, J. Phys. G **11**, 119 (1985).
[22] S. M. Scott, W. D. Hamilton, P. Hungerford, D. D. Warner, G. Jung, K. D. Wunsch, and B. Pfeiffer, J. Phys. G **6**, 1291 (1990).